

# Binding of Phosphatidic Acid to the Protein-Tyrosine Phosphatase SHP-1 as a Basis for Activity Modulation<sup>†</sup>

Carsten Frank,<sup>‡</sup> Heike Keilhack,<sup>‡</sup> Frank Opitz,<sup>§</sup> Olaf Zschörnig,<sup>§</sup> and Frank-D. Böhmer<sup>\*‡</sup>

Research Unit "Molecular Cell Biology", Klinikum der Friedrich-Schiller-Universität Jena, Drackendorfer Strasse 1, D-07747 Jena, Germany, and Institute of Medical Physics and Biophysics, Universität Leipzig, Liebigstrasse 27, D-04103 Leipzig, Germany

Received October 29, 1998; Revised Manuscript Received July 22, 1999

**ABSTRACT:** Activation of the SH2 domain-possessing protein-tyrosine phosphatase SHP-1 by acidic phospholipids as phosphatidic acid (PA) has been described earlier and suggested to participate in regulation of SHP-1 activity toward cellular substrates. The mechanism of this activation is poorly understood. Direct binding of phosphatidic acid to recombinant SHP-1 could be demonstrated by measuring the extent of [<sup>14</sup>C]PA binding in a chromatographic assay, by measuring the extent of binding of SHP-1 to PA-coated ELISA plates or silica beads (TRANSIL), and by spectroscopic assays employing fluorescently labeled PA liposomes. In addition to PA, phosphatidylinositol 3,4,5-trisphosphate (PIP3), dipalmitoylphosphatidylglycerol, phosphatidylinositol 4,5-bisphosphate, and phosphatidylserine (PS) were found to bind to SHP-1, albeit to a lesser extent. A high-affinity binding site for PA and PIP3 was mapped to the 41 C-terminal amino acids of SHP-1. This site was absent from the related protein-tyrosine phosphatase SHP-2 and conferred activation of SHP-1 by PA toward two different substrates at low lipid concentrations. A SHP-1 mutant missing this binding site could, however, still be activated toward phosphorylated myelin basic protein as a substrate at high PA concentrations. This activation is likely to be mediated by a second, low-affinity binding site for PA in the N-terminal part of SHP-1 within the SH2 domains. High-affinity phospholipid binding to the C-terminus of SHP-1 may present a specific mechanism of regulating activity and/or cellular localization.

Protein-tyrosine phosphatases (PTPs)<sup>1</sup> represent a large family of structurally diverse molecules which reverse cellular tyrosine phosphorylations and are therefore considered to be as important for cellular regulation as protein-tyrosine kinases (1, 2). While for many PTPs substrates and exact cellular roles have not been well investigated, the subfamily of PTPs with SH2 domains comprising SHP-1 (PTP1C, HCP) and SHP-2 (PTP1D, syt) (3) has received much attention and multiple cellular binding partners and potential substrates have been identified (for reviews, see refs 1 and 4–7). SHP-2 is widely expressed and seems to fulfill an essential function in the signal transduction of multiple growth factor receptors. SHP-1 may have functions

similar to those of SHP-2 under certain conditions, but in the majority of the experimental systems that were studied, SHP-1 seems to negatively regulate signal transduction of diverse types of receptors (8–16).

An important mechanism for activity regulation of both types of SH2 domain PTPs is their activation as a consequence of recruitment of the SH2 domains by tyrosine-phosphorylated proteins (17–21). A further level of activity regulation may involve phosphorylation on tyrosine or serine residues (22, 23). Finally, activation of both SHP-1 and SHP-2 toward macromolecular substrates by acidic phospholipids has been described (24, 25). In line with these observations, we have previously found that SHP-1 becomes activated toward the autophosphorylated EGF receptor in vitro and in intact cells by PA (13). Thus, SH2 domain PTPs may be modulated in their cellular activities by phospholipids. Regulation of enzyme activity by lipid second messengers is a common phenomenon in signal transduction, with PKC family enzymes as a paradigm (26, 27). Recently, protein kinases activated by the lipid products of phosphoinositide 3-kinases have received much attention (28–32). Also, phosphatidic acid has been shown previously to modulate the activity of enzymes involved in signal transduction, including rolipram-sensitive, cAMP-specific phosphodiesterase isoforms (33), phospholipase D (34), and the protein kinase Raf-1 (35, 36). Raf-1 binds PA via a 35-amino acid segment within the C-terminal domain, and lipid binding is believed to participate in membrane recruitment and enzyme regulation in the proximity of the membrane.

<sup>†</sup> This work was supported by grants from the Sonderforschungsbereich 197 (Projects A9 and A10) of the Deutsche Forschungsgemeinschaft and from the Max-Planck-Society.

<sup>\*</sup> To whom correspondence should be addressed. Fax: +49-3641-304462. E-mail: i5frbo@rz.uni-jena.de.

<sup>‡</sup> Klinikum der Friedrich-Schiller-Universität Jena.

<sup>§</sup> Universität Leipzig.

<sup>1</sup> Abbreviations: BIS-TRIS, bis(2-hydroxyethyl)iminotris(hydroxymethyl)methane; DPE, *N*-[6-(dimethylamino)naphthalenyl-2-sulfonyl]-phosphatidylethanolamine (Dansyl-PE); DPPA, dipalmitoylphosphatidic acid; DPPC, dipalmitoylphosphatidylcholine; DPPG, dipalmitoylphosphatidylglycerol; EGF, epidermal growth factor; ELISA, enzyme-linked immunosorbent assay; LUV, large unilamellar vesicles; MBP, myelin basic protein; MLV, multilamellar vesicles; PA, phosphatidic acid; PBS, phosphate-buffered saline; PC, phosphatidylcholine; PIP2, phosphatidylinositol 4,5-bisphosphate; PIP3, phosphatidylinositol 3,4,5-trisphosphate; pNPP, *p*-nitrophenyl phosphate; PS, phosphatidylserine; PTP, protein-tyrosine phosphatase; pyC10PPC, 1-hexadecanoyl-2-(1-pyrenedecanoyl)-sn-glycerol-3-phosphatidylcholine; SUV, small unilamellar vesicles.

In the course of this study, we sought to better characterize the lipid modulation of SHP-1. We demonstrate with four different methods that SHP-1 can directly bind PA. Two different binding sites with distinct lipid specificity reside in the 41 C-terminal amino acids of the molecule and in the N-terminal part comprising the SH2 domains and hinge domain, respectively. The latter, low-affinity binding site partially overlaps with the SH2 domain phosphopeptide binding site and confers activation of SHP-1 at high lipid concentrations, while the former, which is absent in SHP-2, confers activation at low lipid concentrations.

## EXPERIMENTAL PROCEDURES

**Materials.** The 96-well microtiter plates (ProBind variety) were obtained from Becton Dickinson (Franklin Lakes, NJ). Glutathione Sepharose 4B was purchased from Pharmacia Biotech. Bovine serum albumin (essentially fatty acid free), myelin basic protein (MBP), and *p*-nitrophenyl phosphate (pNPP) were purchased from Sigma. All phospholipids tested and DPE were obtained from Sigma or Avanti Polar Lipids. 1-Hexadecanoyl-2-(1-pyrenedecanoyl)-*sn*-glycero-3-phosphatidylcholine (pyC10PPC) was from Molecular Probes (Eugene, OR). [ $\gamma$ - $^{32}$ P]ATP (111 TBq/mmol) and [ $^{14}$ C]DPPA (5.3 GBq/mmol) were purchased from NEN Life Science Products. LIPIDEX-1000 was from Packard; factor Xa was from Boehringer Mannheim, and antibodies were from Santa Cruz Biotechnology.

**Substrate and Competitor Peptides.** Tyrosine-phosphorylated MBP ([ $^{32}$ P]Y-MBP) was prepared using [ $\gamma$ - $^{32}$ P]ATP and a GST-p60c-src fusion protein following a protocol described previously (37). In brief, a GST-p60c-src fusion protein was obtained by subcloning of the human *c-src-1* gene from the pBA3CS plasmid DNA (38; generously provided by D. Fujita, University of Calgary, Calgary, AB) in frame into the pGEX-5X-2 vector (Pharmacia, Uppsala, Sweden), and the fusion protein was expressed and purified using standard techniques. MBP (5 mg/mL) was phosphorylated by GST-p60c-src (20  $\mu$ g/mL) in a reaction mixture containing 50 mM Tris-HCl (pH 7.5), 10 mM MgCl<sub>2</sub>, 0.1 mM Na<sub>2</sub>EDTA, 1 mM DTT, 0.015% Brij 35, 100  $\mu$ g/mL BSA, and [ $\gamma$ - $^{32}$ P]ATP (100  $\mu$ Ci/ $\mu$ mol) (final concentrations). The incubation was allowed to proceed at 30 °C for 2 h. The reaction was terminated by addition of ice-cold 100% (w/v) trichloroacetic acid to a final concentration of 20% (w/v). The following steps were identical to the published protocol (37).

Peptides DPPHLKYLYLVVSDSK and DPPHLK(p)-YLYLVVSDSK representing the binding site for the SHP-1 N-terminal SH2 domain in the human erythropoietin receptor (14, 18) were obtained from BioTez GmbH (Berlin).

**Expression and Purification of GST Fusion Proteins Representing Different PTPs and PTP Fragments.** cDNAs for SHP-1 and SHP-2 were generously provided by A. Ullrich and R. Lammers (Max-Planck-Institut für Biochemie, Martinsried, Germany). In general, the expression constructs for GST fusion proteins used in this study were obtained by direct subcloning or by cloning of PCR-amplified fragments from constructs containing SHP-1, SHP-2, or SHP-1-SHP-2 chimerical DNA described previously (12) into pGEX-5X vectors (Pharmacia Biotech). Cloning of pGEX-5X-1-SHP-1 and pGEX-5X-1-SHP-1-SH2 has been described previously

(39). Truncation of the last 41 amino acids of the C-terminus of SHP-1 (GST-SHP-1 $\Delta$ tail) was performed using oligonucleotide primers 5'-AAG AAT TCC CCT ACA GAG AGA TGC TGT CC-3' and 5'-TCA GCG GGA GGC CTT GGC ATG-3' to amplify a PCR fragment with a 5'-*Eco*RI site from SHP-1 DNA. The fragment was cloned into pBluescript KS/*Eco*RI/*Sma*I and subcloned in pGEX-5X-1/*Eco*RI/*Not*I. The C-terminal peptide of SHP-1 (GST-SHP-1tail) was obtained from pGEX-5X-1-SHP-1/*Stu*I/*Not*I and cloned into pGEX-5X-3/*Sma*I/*Not*I. GST-SHP-2 was obtained using oligonucleotide primers 5'-AGA TCA AGC TTG GGA GGA ACA TGA CAT CGC GG-3' and 5'-CTA GTC TAG ATC ATC TGA AAC TTT TCT GCT GTT G-3' to amplify a PCR fragment with a 5'-*Hind*III and a 3'-*Xba*I site from SHP-2 DNA. The fragment was cloned into pBluescript KS/*Hind*III/*Xba*I. This construct was sequentially treated with *Not*I, *Pfu* DNA polymerase, and *Hind*III, and the obtained SHP-2 DNA was cloned into pRK5 RS treated with *Xho*I, *Pfu* DNA polymerase, and *Hind*III. The SHP-2 DNA-containing fragment from pRK5 RS/*Eco*RI/*Xho*I was then subcloned into pGEX-5X-1. The construction of the SHP-1-SHP-2 chimera was performed using an existing *Pst*I site in the DNA of SHP-1 and SHP-2 corresponding to the amino acids depicted in Figure 4. All constructs were verified by DNA sequencing.

Expression and purification of the fusion proteins as well as removal of the GST tag with factor Xa and purification of the free SHP-1, SHP-2, and SHP-1 $\Delta$ tail were carried out as described previously (39).

**Binding of [ $^{14}$ C]DPPA to SHP-1.** [ $^{14}$ C]DPPA and unlabeled DPPA were dried from chloroform solutions under a stream of nitrogen and redissolved in binding buffer [20 mM imidazole (pH 7.0), 1 mM EDTA, and 1 mM dithiothreitol]. Vesicles were prepared by sonication for 0.5–2 min until the solution became clear. Binding of [ $^{14}$ C]DPPA to GST-SHP-1 was performed in 100  $\mu$ L of a solution containing 1  $\mu$ M GST-SHP-1 or GST and 0.2  $\mu$ Ci of [ $^{14}$ C]DPPA (final concentration of 13  $\mu$ M) in the presence or absence of a 40-fold excess of unlabeled DPPA in binding buffer overnight at 4 °C. The mixtures were then chromatographed on a 1 cm  $\times$  2.5 cm column of LIPIDEX-1000, previously equilibrated with binding buffer at 4 °C. Protein-bound [ $^{14}$ C]DPPA was eluted in the void volume. [ $^{14}$ C]DPPA bound to the column was then eluted with methanol. Fractions (0.5 mL) were collected, and radioactivity in aliquots of the fractions was measured by liquid scintillation counting.

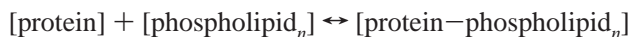
**Lipid Binding Assay by ELISA.** The binding of GST-SHP-1 to phospholipid-coated 96-well microtiter plates was performed following the protocol described by Gosh et al. (36). In brief, phospholipids (0–5  $\mu$ g per well) dissolved in methanol were allowed to bind overnight at 4 °C. All the following ELISA steps were performed at room temperature. The wells were blocked with 3% bovine serum albumin in PBS [20 mM NaH<sub>2</sub>PO<sub>4</sub>, 80 mM Na<sub>2</sub>HPO<sub>4</sub>, and 100 mM NaCl (pH 7.5)] for 1 h. GST fusion proteins diluted in PBS (pH 7.5) containing 0.3% bovine serum albumin were added to the wells, and binding was allowed for 1 h. Bound GST fusion proteins were detected by employing anti-GST rabbit polyclonal antiserum (1/500) and a goat anti-rabbit IgG-alkaline phosphatase conjugate (1/2000). The plate was washed with PBS containing 0.1% Tween 20 (three times for 5 min each) after incubation with GST fusion proteins

and antibodies. After excess secondary antibody had been washed off, a 10 mg/mL solution of pNPP in buffer [10 mM Tris-HCl (pH 9.5), 100 mM NaCl, and 5 mM MgCl<sub>2</sub>] was added to the wells for color development. The reaction was terminated by the addition of 33 mM EDTA, and the resulting absorbancies were quantitated at 405 nm on an ELISA plate reader. Controls including GST-SHP-1 but without secondary antibodies yielded background values identical to controls without GST fusion proteins. Also, the total amounts of SHP-1-GST fusion protein used in these assays had virtually no activity under the conditions of alkaline phosphatase assay.

**Binding of SHP-1 to TRANSIL.** Silica gel coated with a single phospholipid bilayer (TRANSIL) containing PC (egg yolk) and PA (from egg yolk PC) (4/1, w/w) was purchased from NIMBUS (Leipzig, Germany). The binding of GST-SHP-1 to TRANSIL was performed by following the manufacturer's instructions. Five hundred microliters of a solution containing 0.5  $\mu$ M GST-SHP-1 and various amounts of a TRANSIL dispersion (lipid concentration of 0–2 mM) in buffer [10 mM Tris-HCl (pH 7.4), 1 mM EDTA, and 100 mM NaCl] was incubated at room temperature by being gently shaken for 1 h. After incubation, the mixture was centrifuged (5 min at 10000g), and 100  $\mu$ L of the supernatant was analyzed by SDS-PAGE. The amount of protein remaining in the supernatant was quantified densitometrically.

**Evaluation of Interactions between Lipid and SHP-1 by Fluorescence Spectroscopy.** Multilamellar phospholipid vesicles (MLV) were prepared using the method of Bangham (40). DPE was mixed with the phospholipids in chloroform at a phospholipid/DPE molar ratio of 200–300 before evaporation. The lipid was initially dried from chloroform, subsequently dispersed in buffer solution [10 mM HEPES and 100 mM NaCl (pH 7.4)], and shaken at a temperature above the gel-to-liquid-crystalline transition temperature for 10 min. Large unilamellar vesicles (LUV) were then prepared via five freezing–thawing cycles of MLV and following extrusion (five times) through 0.1  $\mu$ m Nucleopore filter membranes using an extruder (Lipex Biomembranes, Vancouver, BC) at 30 °C. Alternatively, small unilamellar vesicles (SUV) containing 5% pyC10PPC were prepared by sonicating MLV (2 min under temperature control). The fluorescence assays were carried out on a Jobin Yvon Spex Fluoro Max-2 spectrofluorimeter (Edison, NJ) using quartz cuvettes equipped with a magnetic stirrer. Vesicles were suspended in 1.0 mL of buffer at concentrations of about 80  $\mu$ M for the DPE assay, and 2  $\mu$ M for the pyC10PPC assay. The recording started after the system had reached equilibrium (about 3–5 min). Appropriate aliquots of aqueous protein stock solutions were added to the vesicle suspension and continuously stirred. The experiments were performed at 37 °C. For measurements with DPE-containing LUV, the excitation wavelength was 340 nm, and the emission was measured in the range of 400–600 nm. For measurements with the pyC10PPC-containing SUV, the excitation wavelength was 340 nm. The emission spectra were measured from 360 to 500 nm. For the evaluation of the data in the latter case, the excimer/monomer ratio (*E/M*) of pyC10PPC was used. For this purpose, the emission intensities at 378 and 475 nm were calculated. Protein-SUV interaction results in changes in the *E/M* ratio.

**Calculation of Binding Constants.** Theoretical binding isotherms were calculated from spectroscopic data on the basis of a model in which protein molecules are considered ligands that bind independently to sites on the phospholipid vesicles with an apparent association constant  $K_A$  ( $=1/K_D$ ); each site consists of *n* phospholipid molecules.



The observed change  $\Delta$  in *E/M* divided by the maximal change  $\Delta_{\text{max}}$  was taken to be proportional to the number of sites occupied by the protein divided by the total number of sites.

$$[\text{protein-phospholipid}]_n / [\text{phospholipid}]_{n,\text{total}} = \Delta / \Delta_{\text{max}}$$

A simple quadratic equation was solved to give [protein-phospholipid]<sub>n</sub>.  $\Delta$  is obtained from

$$\Delta = \Delta_{\text{max}} [\text{protein-phospholipid}]_n / [\text{phospholipid}]_{n,\text{total}}$$

Protein/phospholipid ratios were calculated by assuming that 50% of the total phospholipid was accessible to the protein. Data were fitted using a nonlinear regression algorithm in a Sigmaplot 4.0 spreadsheet.

An analogous procedure was used to calculate apparent dissociation constants from data from the ELISA binding assay, assuming in this case that 100% of the coated phospholipid was accessible to protein and that the coated lipid was homogeneously dispersed in the incubation volume.

**PTP Assays.** PTP assays were performed with either pNPP (10 mM) or radioactively tyrosine-phosphorylated MBP ([<sup>32</sup>P]Y-MBP, approximately 2  $\mu$ M) in the presence or absence of 0.01–50  $\mu$ g/mL phospholipids at 30 °C for the periods of incubation time given in the figure legends. In the case of the pNPP assay, the reactions were terminated by the addition of 66 mM NaOH and the activity was quantitated at 405 nm on an ELISA plate reader. The following buffers were used for adjustment of the different pH values: pH 5.1 and 5.4, 100 mM sodium acetate; pH 5.8 and 6.3, 100 mM BIS-TRIS; and pH 7.4, 100 mM HEPES. In addition, all buffers contained 150 mM NaCl, 1 mM EDTA, and 1 mM  $\beta$ -mercaptoethanol. For estimation of enzyme kinetic parameters, SHP-1 (50 nM) was subjected to assays with pNPP as described above in the absence or presence of DPPA (25  $\mu$ g/mL), varying the pNPP concentration from 1 to 500 mM. The data were evaluated employing the program Enzyme Kinetics (Trinity Software, Campton, NH). Activation measurements using the synthetic phosphopeptide DPPHLK(p)YLYLVVSDSK were carried out as described previously (39).

The assays with [<sup>32</sup>P]Y-MBP were performed in buffer containing 25 mM imidazole (pH 7.2), 1 mg/mL bovine serum albumin, and 0.1%  $\beta$ -mercaptoethanol. The reactions were terminated with 15% trichloroacetic acid; the samples were centrifuged (10 min at 15000g), and the released [<sup>32</sup>P]-phosphate in the supernatant was quantified by liquid scintillation counting.

## RESULTS

**SHP-1 Directly Binds Phosphatidic Acid.** Previous findings for the activation of SHP-1 by acidic phospholipids suggested that SHP-1 possesses a binding site(s) for such lipids (13,



24). To assess the presence of putative binding sites, we first tested the binding of [ $^{14}$ C]dipalmitoylphosphatidic acid (DPPA) to SHP-1. A GST fusion protein of SHP-1 was incubated with [ $^{14}$ C]-labeled DPPA in the absence or presence of an excess of unlabeled DPPA. The mixtures were separated over a hydrophobic gel chromatography matrix (LIPIDEX-1000). Any [ $^{14}$ C]DPPA bound to SHP-1 is expected to elute in the void volume in this setting, whereas unbound [ $^{14}$ C]DPPA is retarded and can be eluted with methanol. As shown in Figure 1A, [ $^{14}$ C]DPPA can be recovered in the void volume with GST-SHP-1 and is displaced by an excess of DPPA. GST alone exhibits only a background level of binding to [ $^{14}$ C]DPPA. Further evidence for direct binding of SHP-1 to PA was obtained using beads (TRANSIL) coated with a PA (20%)/PC (80%) bilayer for a binding assay. As shown in Figure 1B, GST-SHP-1 can be depleted from solution in a dose-dependent manner with these beads, whereas beads coated with PC alone did not bind GST-SHP-1. To further establish the binding of PA to SHP-1, we employed an assay previously used to demonstrate binding of phospholipids to Raf-1 kinase (36). DPPA was coated onto ELISA plates; binding of GST-SHP-1 to the coated lipid was allowed, and the bound protein was detected by an ELISA with anti-GST antibodies. As depicted in Figure 2A, GST-SHP-1 binds in a time-dependent manner to DPPA. No binding can be observed to ELISA plates which were not coated with DPPA or for free GST (Figure 2B). The binding depends in a saturable manner on the amount of coated DPPA (Figure 2C) and the amount of GST-SHP-1 (Figure 2D). Finally, interaction of SHP-1 with PA could also be demonstrated by fluorescence spectroscopy employing fluorescently labeled PA liposomes (Figure 3). In the first experimental setup, we tested selected lipids for their interaction with SHP-1 using large unilamellar liposomes containing DPE as a fluorescent probe. The wavelength of the maximum of the emission spectrum depends on the dielectric properties of the environment of the probe. Protein interaction of the liposomes leads to formation of dehydrated areas in the proximity of the protein and in turn to lowering of the dielectric constant. As a consequence, the maximum of the emission spectrum is shifted to a lower wavelength (41). This method has been extensively employed previously to characterize lipid-annexin interactions (42). In Figure 3A, the emission wavelength shift of DPE-containing PA, PS, and PC LUV is shown as a function of protein concentration. Clearly, interaction of both GST-SHP-1 and SHP-1 but not free GST with PA liposomes could be detected with this technique, while negligible interaction occurred with PS or PC liposomes (Figure 3A). The wavelength shift occurred apparently at lower concentrations with GST-SHP-1 than with SHP-1. This may indicate steric differences in the accessibility of the lipid binding site(s) in the two different proteins; however, given the relatively low sensitivity of this method, such quantitative differences are difficult to interpret. An alternative, more sensitive technique utilizes the fluorescent probe 1-hexadecanoyl-2-(1-pyrenedecanoyl)-sn-glycero-3-phosphatidylcholine (pyC10PPC) incorporated in PA small unilamellar vesicles (SUV). Interaction of GST-SHP-1 with these vesicles leads to concentration-dependent alterations in the ratio of emission intensities at 378 (excimer) and 475 nm (monomer) of pyC10PPC (Figure 3B), while

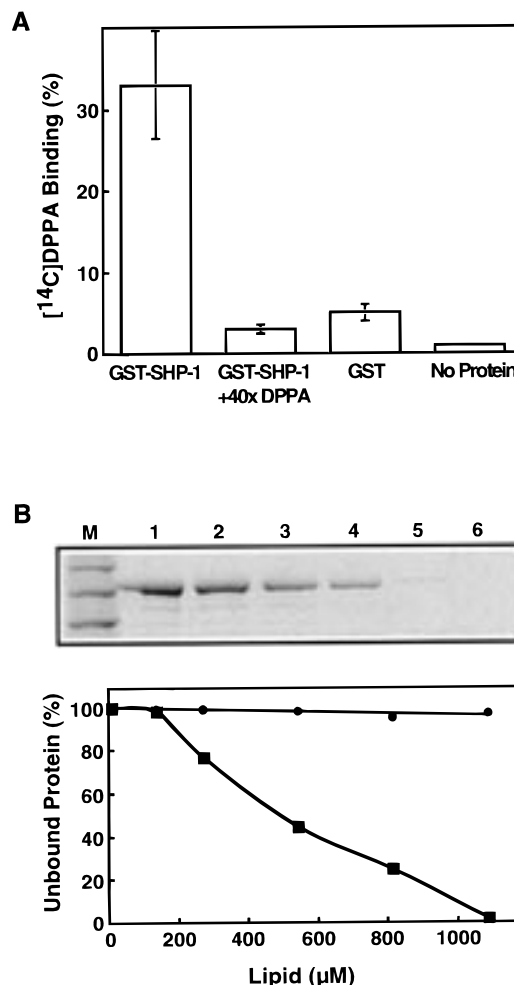


FIGURE 1: Binding of phosphatidic acid to SHP-1. (A) Ten micrograms of GST-SHP-1 was incubated with [ $^{14}$ C]dipalmitoylphosphatidic acid ([ $^{14}$ C]DPPA, 13  $\mu$ M, ca.  $4 \times 10^5$  dpm) in the presence or absence of a 40-fold excess of DPPA (as indicated) at 4  $^{\circ}$ C overnight at pH 7.0. The mixture was separated over a hydrophobic gel chromatography (LIPIDEX-1000) column, and the radioactivity in the void volume and the radioactivity bound to the column and subsequently eluted with methanol were determined. The radioactivity eluting in the void volume is presented as a percentage of the total radioactivity eluted from the column. Corresponding control assays were performed for free GST and in the absence of any protein, as indicated. (B) Binding of SHP-1 to phosphatidic acid-coated beads. Different amounts of beads (TRANSIL) coated with a bilayer of either PA (from egg yolk)/PC (20%/80%) or PC only were incubated with GST-SHP-1 (50  $\mu$ g/mL) for 1 h at room temperature under end-over-end rotation. The beads were centrifuged, and the GST-SHP-1 remaining in the supernatant was detected by SDS-PAGE. (Upper panel) Representative experiment with PA/PC beads. PA/PC (1/4) concentrations are (1) 136, (2) 272, (3) 544, (4) 816, (5) 1088, and (6) 1632  $\mu$ M. (Lower panel) Quantification of GST-SHP-1 remaining in the supernatant as revealed by densitometric scanning of a representative binding experiment with PA/PC (■) or PC (●).

no interaction occurs for free GST with PA SUV or for GST-SHP-1 with PC SUV. Fitting of these data assuming a simple model of SHP-1-PA interaction described in Experimental Procedures reveals an apparent dissociation constant of  $4.33 \times 10^{-8}$  mol/L.

**Specificity of Phospholipid Binding to SHP-1.** Different lipids were compared for their capacity to bind SHP-1, using the ELISA technique. Equal amounts of lipids were coated onto the plates, and binding of GST-SHP-1 was evaluated.

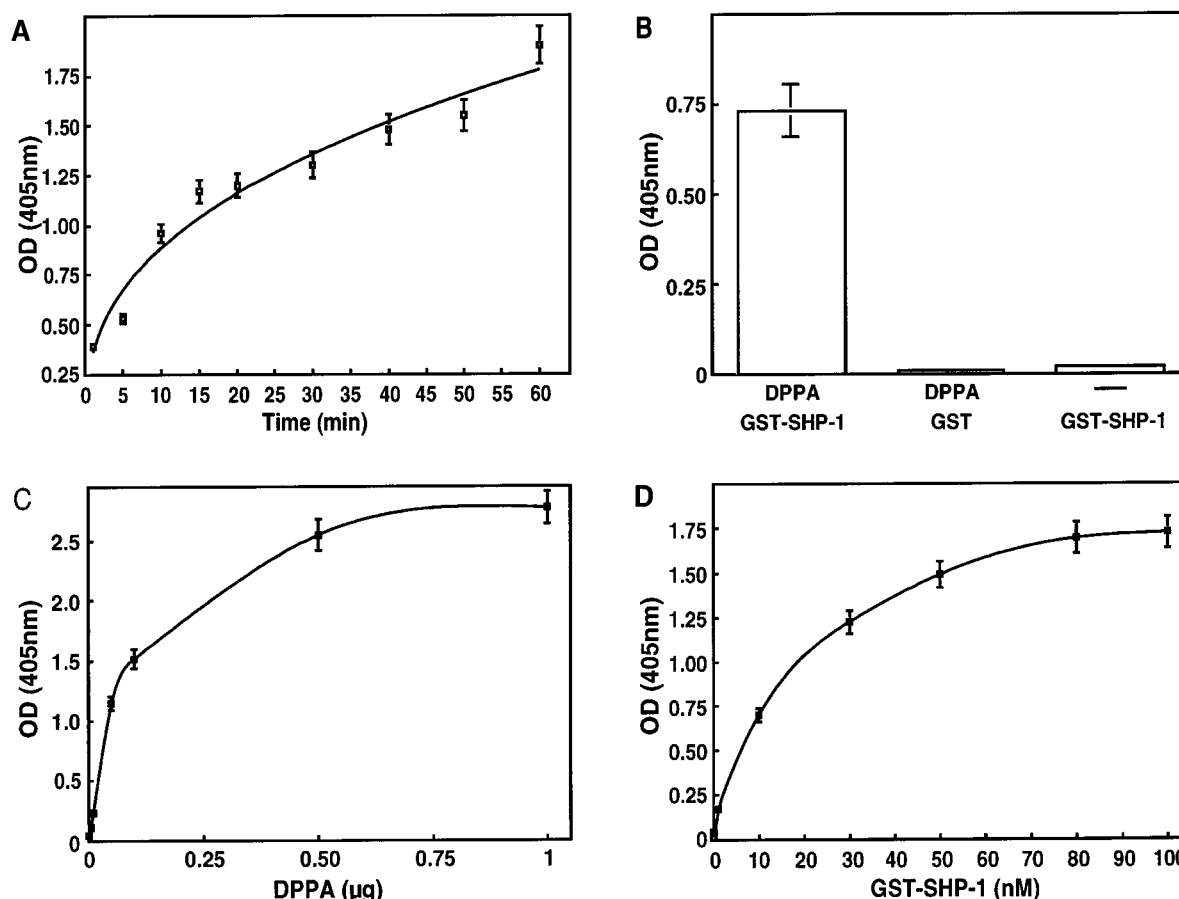


FIGURE 2: Binding of SHP-1 to dipalmitoylphosphatidic acid as determined by ELISAs. (A) Wells of an ELISA plate were coated with 100 ng/well DPPA and were subsequently blocked by incubation with BSA. Thereafter, the wells were incubated with 25 nM GST-SHP-1 at room temperature for different periods of time, as indicated. The wells were washed, and GST in the wells was detected with an ELISA employing anti-GST antibodies. (B) The assay was performed as described for panel A with 50 nM GST-SHP-1 or GST alone. The wells were coated with DPPA (100 ng/well) or treated with solvent only (control). Binding was allowed to occur for 1 h. (C) The assay was performed as described for panel A with 50 nM GST-SHP-1 as a binding partner for different amounts of coated DPPA. (D) Concentration dependence of GST-SHP-1 binding to DPPA (5  $\mu$ g/well), otherwise performed as described for panel A.

As shown in Table 1, the strongest binding of GST-SHP-1 was obtained with DPPA. Significant binding was also observed for PA from egg yolk lecithin, DPPG (not shown), and phosphatidylinositol 4,5-bisphosphate, and interestingly, a rather strong binding was observed with phosphatidylinositol 3,4,5-trisphosphate. Reproducibly, very low-level binding occurred also to PS. Negligible binding could be detected with PC, DPPC, or phosphatidylinositol 4-phosphate (not shown). This specificity assay may be partially biased by the different coating efficiencies of the various lipids; however, a clear preference for binding of SHP-1 to PA over PS and no binding to PC was likewise observed in the interaction studies with fluorescently labeled liposomes, described above.

**A PA Binding Site in the C-Terminal Tail of SHP-1.** To localize the PA binding site(s) on the SHP-1 protein, different SHP-1 deletion mutants were generated and expressed as GST fusion proteins. For comparison, the related PTP SHP-2 and SHP-1-SHP-2 chimerical proteins with exchanged C-terminal parts were also included in the analysis (Figure 4). The various proteins were tested for their interaction with DPPA, PA, PS, PIP2, and PIP3 in the ELISA. The results are shown in Table 1. A GST fusion protein harboring the last 43 amino acids of SHP-1 (GST-SHP-1tail) exhibited lipid binding characteristics almost identical to those of full-

length SHP-1, suggesting that much of the lipid binding capacity of SHP-1 resides in the C-terminus. In agreement with this assumption, lipid binding was lost with the corresponding SHP-1 variant with a truncated tail (GST-SHP-1 $\Delta$ tail). In contrast to GST-SHP-1, GST-SHP-2 exhibited only a comparatively low level of binding of all lipids tested. A SHP-1-SHP-2 chimera with the tail of SHP-1 replaced by the one of SHP-2 (GST-SHP-1-SHP-2tail) bound no lipid, like GST-SHP-1 $\Delta$ tail. In contrast, the reverse SHP-2-SHP-1 chimera (GST-SHP-2-SHP-1tail) exhibited again a binding profile very similar to that of GST-SHP-1tail. In summary, these data support the presence of a lipid binding site in the C-terminal tail of SHP-1 which does not exist in SHP-2 with a clear preference for DPPA, PIP3, and PA over PIP2 and PS. Interestingly, another fragment of SHP-1 containing the SH2 domains and a short stretch of amino acids ("hinge") intervening the SH2 domains and the catalytic domain (GST-SHP-1SH2) exhibited a low level of binding to PA and PS in the ELISA, indicating the presence of a second, lower-affinity lipid binding site in this part of the SHP-1 molecule (Table 1). This binding site seems to be inaccessible under the standard assay conditions in the ELISA in GST-SHP-1 $\Delta$ tail or GST-SHP-1-SHP-2tail but may contribute to lipid binding in full-length GST-SHP-1. In fact, lipid binding to GST-SHP-1 $\Delta$ tail similar to the

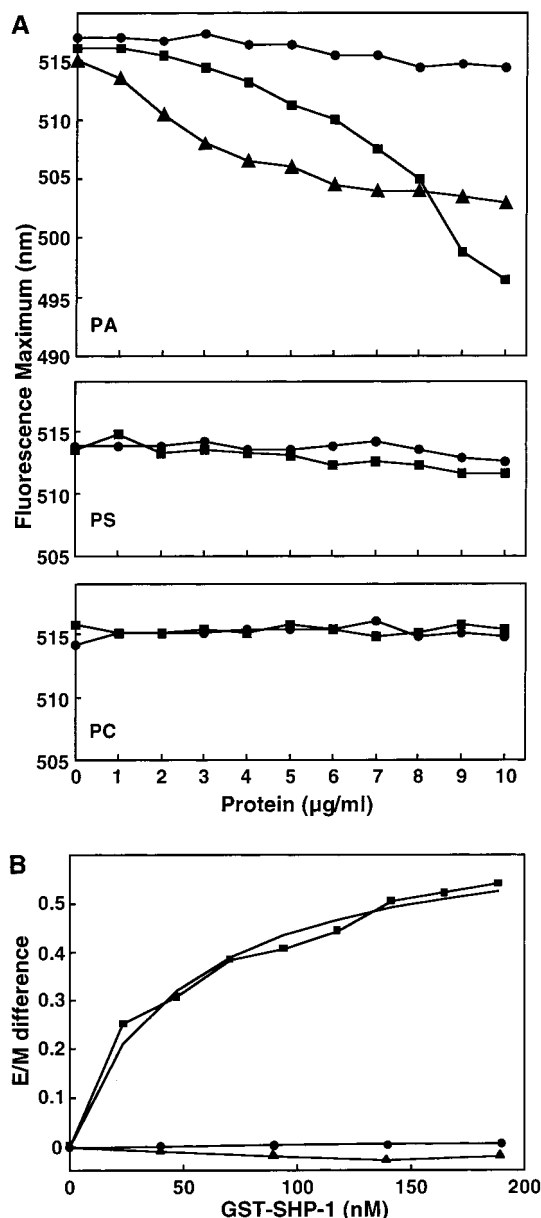


FIGURE 3: SHP-1 interaction with fluorescently labeled phosphatidic acid liposomes. (A) Liposomes with a diameter of  $\leq 100$  nm (LUV) were prepared from the indicated lipids and 1% DPE as described in Experimental Procedures. Fluorescence spectra were recorded at 37 °C in the presence of GST alone (●), GST-SHP-1 (■), or free recombinant SHP-1 (▲). Protein interaction with the liposomes is indicated by a concentration-dependent shift of a maximum of fluorescence at approximately 515 nm in the absence of protein to a lower wavelength. (B) SUV from phosphatidic acid (■ and ●) or phosphatidylcholine (▲) containing 5% pyC10PPC were prepared and exposed to different concentrations of GST-SHP-1 (■ and ▲) or free GST (●). Fluorescence spectra were recorded, and excimer/monomer (*E/M*) ratios were determined as described in Experimental Procedures. Interaction of the proteins with the SUV results in a concentration-dependent change in the *E/M* ratios, which is plotted as a function of protein concentration. For interaction of GST-SHP-1 with the PA liposomes, the data were fitted and the theoretical curve according to the fit is also depicted (no symbols).

binding of GST-SHP-1SH2 in the ELISA could be obtained upon elevation of the salt concentration (not shown). It seems also tempting to speculate that lipid binding to GST-SHP-2 occurs with the SHP-2 SH2 domain/hinge part, since the tail of SHP-2 has no lipid binding capacity.

Table 1: Binding of Lipids to SHP-1, SHP-2, and SHP-1 Mutants<sup>a</sup>

protein	DPPA	PA	PS	PIP2	PIP3
GST-SHP-1	1.00	0.27	0.05	0.20	0.56
GST-SHP-2	0.24	0.09	0.07	0.04	0.06
GST-SHP-1-SHP-2tail <sup>b</sup>	0.01	0.02	0.01	0.01	0.00
GST-SHP-2-SHP-1tail	1.20	0.50	0.18	0.37	0.80
GST-SHP-1Δtail <sup>b</sup>	0.06	0.02	0.01	0.01	0.01
GST-SHP-1tail	1.18	0.39	0.04	0.20	0.55
GST-SHP-1SH2	0.06	0.11	0.11	0.04	0.04
control (GST)	0.01	0.01	0.00	0.01	0.00

<sup>a</sup> Binding assays were carried out with the different recombinant GST fusion proteins depicted in Figure 4 as described in the legend of Figure 2. Values are normalized to binding of GST-SHP-1 to DPPA (1.0).

<sup>b</sup> Lipid binding similar to that of GST-SHP-1SH2 is observed for these mutants at elevated salt concentrations.

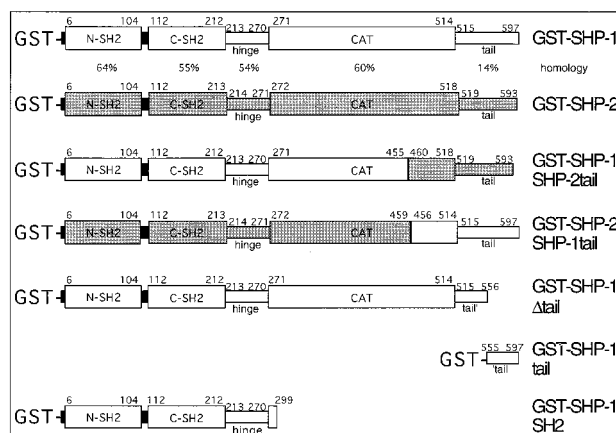


FIGURE 4: Structure and designation of SHP-1 and SHP-2 constructs used for mapping of the lipid binding sites. The depicted structural elements are N- and C-terminal SH2 domains (N-SH2 and C-SH2, respectively), the “hinge” sequence between the C-terminal SH2 domain and the catalytic domain (CAT), and the C-terminal “tail” structure. Percentages of sequence identity at the amino acid level are depicted for the different domains of SHP-1 and SHP-2. The amino acid numbering is for SHP-1 as described in ref 53 and for SHP-2 as described in ref 21.

To further characterize the two lipid binding sites in SHP-1, the time and concentration dependencies of lipid binding were characterized for GST-SHP-1tail and GST-SHP-1SH2. Binding of both proteins was saturable with time, reaching a plateau after incubation for approximately 60 min (not shown). With respect to concentration dependence, GST-SHP-1tail behaves very much like full-length GST-SHP-1 (Figure 5A,B; compare to Figure 2), indicating again that much of the lipid binding observed with the full-length enzyme is mediated via the C-terminal tail. Analysis of GST-SHP-1tail in the binding assay with pyC10PPC-labeled liposomes also revealed saturable binding (not shown) with an apparent dissociation constant of  $23.3 \times 10^{-8}$  mol/L, an affinity somewhat lower than that for the full-length enzyme. GST-SHP-1SH2 also bound to PA in a saturable manner (Figure 5C,D); however, saturation required much higher concentrations of PA (Figure 5C) or protein (Figure 5D). The calculation of apparent dissociation constants from these data requires a number of assumptions (see Experimental Procedures) which makes direct comparison with the absolute values derived from the fluorescence measurements difficult but allows comparison of binding characteristics for the different SHP-1 variants. Calculations yielded values of  $1.34 \times 10^{-8}$  mol/L for the full-length enzyme (data from Figure

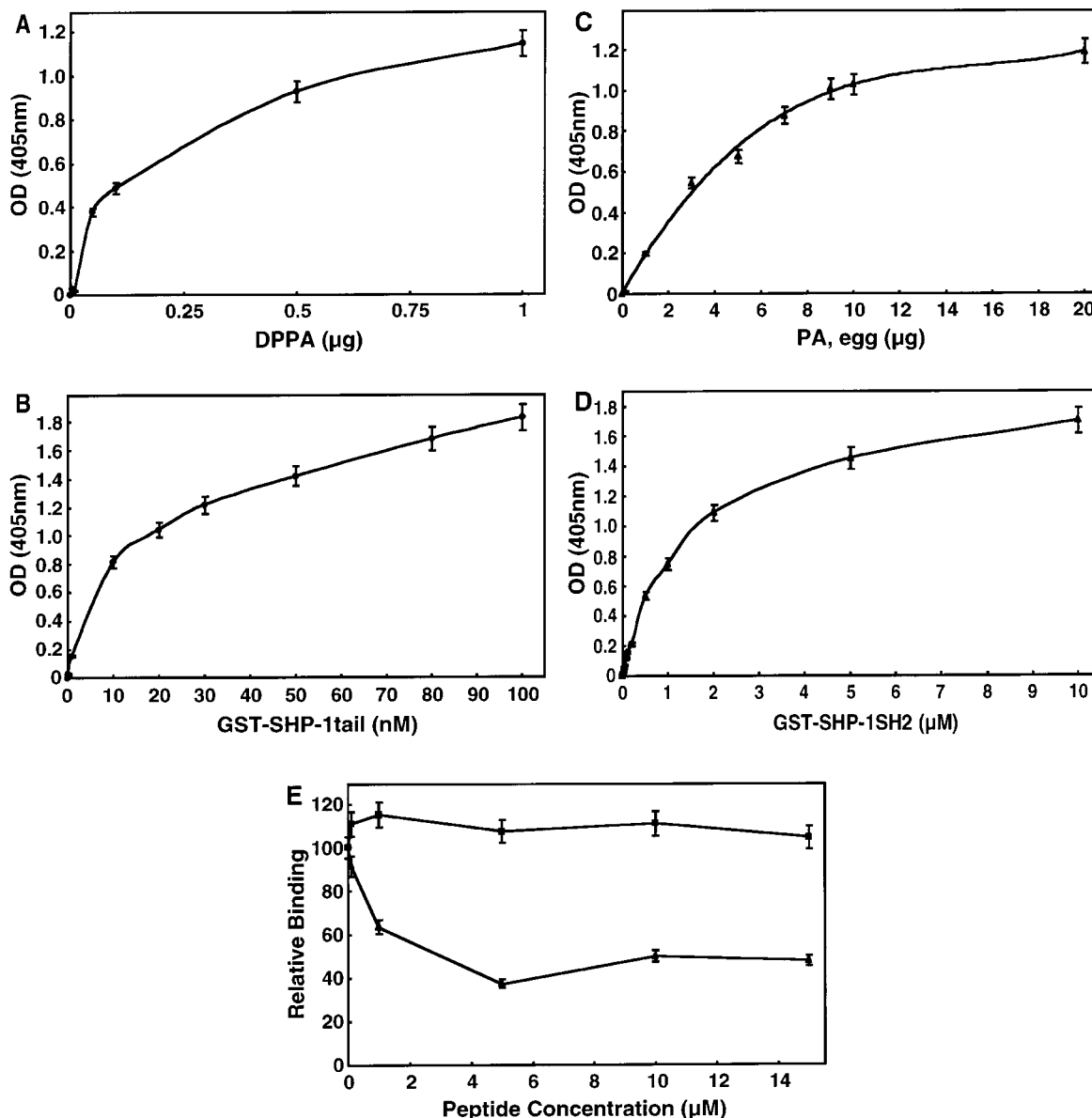


FIGURE 5: Binding of SHP-1 fragments to phosphatidic acid as determined by ELISAs. Wells of an ELISA plate were coated with DPPA (A and B) or PA (C and D) and were subsequently blocked by incubation with BSA. Binding of a GST fusion protein containing the 43 C-terminal amino acids of SHP-1 (A and B, GST-SHP-1tail) or of a GST fusion protein containing the SHP-1 SH2 domains (C and D, GST-SHP-1SH2) was assessed as described in the legend of Figure 2. (A) The assay was performed with 50 nM GST-SHP-1tail as the binding partner for different amounts of coated DPPA. (B) Concentration dependence of GST-SHP-1tail binding to DPPA (5 μg/well). (C) The assay was performed with 100 nM GST-SHP-1SH2 as the binding partner for different amounts of coated PA. (D) Concentration dependence of GST-SHP-1SH2 binding to PA (5 μg/well). (E) Competition of lipid binding to GST-SHP-1SH2 by a tyrosine-phosphorylated peptide. Binding of GST-SHP-1SH2 (100 nM) to PA (10 μg/well) was performed in the presence of different concentrations of a peptide representing the binding site for SHP-1 in the human erythropoietin receptor in the nonphosphorylated (■) or phosphorylated (▲) form. Relative binding is presented compared to control without peptides (100%). When the peptide concentration was further increased up to 100 μM, the level of binding in the presence of the nonphosphorylated form increased up to values 2-fold greater than control values, probably because of physicochemical effects. Still, the level of binding in the presence of the phosphorylated peptide remained at only 50% of these values (not depicted).

2D),  $1.47 \times 10^{-8}$  mol/L for GST-SHP-1tail (Figure 5B), and  $1.48 \times 10^{-6}$  mol/L for GST-SHP-1SH2 (Figure 5D) in this assay. Thus, again, GST-SHP-1tail binds in a manner similar to, and possibly somewhat weaker than, that of the full-length enzyme, whereas GST-SHP-1SH2 exhibits an affinity that is about 2 orders of magnitude lower than that of the C-terminal binding site.

The SH2 domains of SHP-1 are known to bind tyrosine-phosphorylated peptides with high affinity which leads to activation of the enzyme. We therefore tested whether binding of PA and a phosphopeptide to GST-SHP-1SH2

would be competitive. Indeed, a phosphopeptide from the human erythropoietin receptor representing the binding site for the SHP-1 N-terminal SH2 domain (14, 18) competed with the binding of GST-SHP-1SH2 to PA in the ELISA, reducing the level of binding to approximately 50% at 1–5 μM and above, while the nonphosphorylated peptide exhibited no competition (Figure 5E). Thus, the PA binding site in GST-SHP-1SH2 probably overlaps with the binding site for the phosphopeptide in the N-terminal SH2 domain.

*Relation of PA Binding and SHP-1 Activity Modulation by PA.* Knowing lipid binding characteristics of SHP-1, we



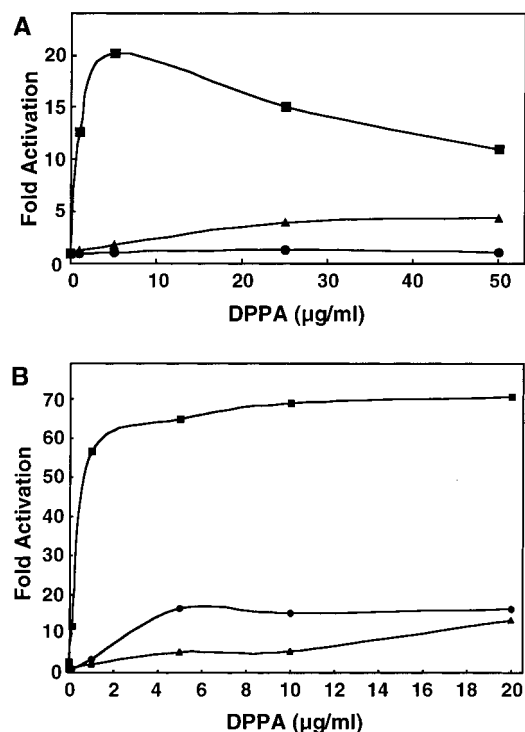


FIGURE 6: Effect of phosphatidic acid on the activity of SHP-1, SHP-2, and SHP-1Δtail against two different substrates. (A) SHP-1 (25 nM, ■), SHP-1Δtail (25 nM, ▲), or SHP-2 (300 nM, ●) was incubated at pH 6.3 with 10 mM pNPP in the presence of different concentrations of DPPA for 2 h at 30 °C. The reaction was quenched by addition of NaOH, and the absorption at 405 nm was recorded as a measure of PTP activity. The activity in the absence of DPPA was normalized to 1.0. (B) SHP-1 (■), SHP-1Δtail (▲), and SHP-2 (●) (25 nM each) were incubated with tyrosine-phosphorylated myelin basic protein ([<sup>32</sup>P]Y-MBP, approximately 2 μM) in the absence or presence of different amounts of DPPA at pH 7.2 for 30 s at 30 °C. The reaction was terminated with TCA, and the amount of released <sup>32</sup>P was determined. The activity of all enzyme variants in the absence of PA was normalized to 1.0.

explored the potential importance of the assigned binding sites for the previously described modulation of SHP-1 activity by PA. The activities of SHP-1, of the SHP-1 variant with C-terminal deletion of 41 amino acids, and of SHP-2 were measured against two different substrates, pNPP and [<sup>32</sup>P]Y-MBP, and the effect of PA was analyzed. For these assays, the respective recombinant PTP variants were analyzed not as GST fusion proteins but in their free form, since GST fusion is known to result in artificial activation of SHP-1. DPPA activated SHP-1 toward pNPP in a concentration- and pH-dependent manner (Figure 6A and not shown). Activation could be detected in the pH range of 5.8–7.4, whereas no activation could be observed at pH 5.1 or 5.4. At pH 5.8–7.4, maximal activation was already detectable with 5–10 μg of DPPA/mL, and half-maximal activation was reached with 0.5–1 μg of DPPA/mL, i.e., approximately 1 μM. High concentrations (25–50 μg/mL) eventually inhibited activity (Figure 6A). The activation by DPPA was the consequence of lowering the  $K_m$  (approximately 50 mM in the presence of DPPA vs approximately 225 mM in its absence at pH 6.3), while the  $V_{max}$  was not increased in the presence of DPPA. In contrast to DPPA, little activation of SHP-1 was seen in this assay with PA from egg yolk lecithin, or PS (not shown). Interestingly, deletion of the 41 C-terminal amino acids of SHP-1 did not change significantly

the activity of the resulting PTP derivative SHP-1Δtail toward pNPP at any of the pH values that were tested, but rendered this variant refractory to DPPA activation (Figure 6A). Likewise, SHP-2 could not be activated toward pNPP with DPPA (Figure 6A). The extent of activation of SHP-1 and SHP-1Δtail toward pNPP by the synthetic phosphopeptide from the erythropoietin receptor sequence representing the SHP-1 binding site was similar (10.8- and 8.7-fold, respectively, at pH 7.4 with 100 μM phosphopeptide). Thus, deletion of the C-terminal lipid binding site does apparently not alter susceptibility to regulation by SH2 domain occupation. Similar experiments were carried out with [<sup>32</sup>P]Y-MBP as a substrate, phosphorylated by using p60c-src. Toward this substrate, SHP-1 could be strongly activated with PA already at concentrations of 0.1 μg/mL (approximately 0.15 μM), and activation was almost maximal with 1 μg/mL PA (approximately 1.5 μM) (Figure 6B). The SHP-1 variant with the deletion of 41 C-terminal amino acids (SHP-1Δtail) and SHP-2 were affected by these concentrations of PA to a much lesser extent (Figure 6B). At higher PA concentrations (5–20 μg/mL, i.e., approximately 7–30 μM), SHP-1Δtail and SHP-2 were also significantly activated toward [<sup>32</sup>P]Y-MBP. PIP3 also activated SHP-1 toward [<sup>32</sup>P]Y-MBP, albeit to a lesser extent than PA (not shown). These data are consistent with a role of the C-terminal high-affinity lipid binding site in activity regulation of SHP-1 by PA and PIP3.

## DISCUSSION

Both hitherto known SH2 domain PTPs SHP-1 and SHP-2 have previously been shown to become activated against different macromolecular substrates by acidic phospholipids (24, 25). This activation has been proposed to contribute to PTP activity in proximity to cellular membranes. Also, data obtained for activation of SHP-1 toward the EGF receptor by PA in vitro and in intact cells led us to propose that lipid modulation of SHP-1 activity may be physiologically relevant for regulation of EGF receptor signaling (13). To date, little was known about the mechanistic basis for SHP-1 or SHP-2 activation by phospholipids. Here we demonstrate that SHP-1 can directly bind acidic phospholipids. One high-affinity binding site could be narrowed to the 41 C-terminal amino acids of SHP-1. It exhibits a preference for DPPA, PIP3, and PA over other phospholipids, does not exist in SHP-2, and confers activation of SHP-1 by PA toward pNPP and [<sup>32</sup>P]Y-MBP. Apparent dissociation constants of approximately 0.04 μM for the full-length enzyme and of 0.23 μM for the isolated C-terminal fragment were obtained from binding studies with fluorescently labeled PA-containing SUV. It is possible that the apparently higher affinity of the full-length enzyme is related to the presence of a second, low-affinity binding site in this protein (see below), which contributes to the total binding. The dissociation constants are in reasonable agreement with PA concentrations of 0.15–1 μM resulting in half-maximal SHP-1 activation. Similar dissociation constants and effective lipid concentrations were observed for the binding of phosphatidylinositol 4-phosphate to the dynamin pleckstrin homology domain (43), the binding of phosphatidylinositol 4,5-bisphosphate to an inward rectifier potassium channel (44), the activation of cAMP-specific phosphodiesterase by phosphatidic acid (45), and the activation of protein kinase B by PIP3 (31).



A second site which binds several acidic phospholipids to a similar extent but with an about 2 order of magnitude lower affinity resides in the N-terminal part of SHP-1, comprising the SH2 domains and the hinge domain. In SHP-1 variants with a deleted C-terminus or with the C-terminus of SHP-2, this binding site seems to be cryptic and can be detected via ELISA-type binding studies only at elevated salt concentrations, but becomes accessible in SH2 domain-hinge constructs. A phosphopeptide which is known to bind to the SHP-1 N-terminal SH2 domain can partially compete with PA binding to this site. It is therefore likely that low-affinity PA binding to SHP-1 occurs at least partly within the N-terminal SH2 domain. A similar binding site seems to exist in SHP-2, and the obtained data suggest that this site confers susceptibility of both enzymes for activation toward the macromolecular substrate [ $^{32}$ P]Y-MBP at high PA concentrations. Structural models for SHP-1 and SHP-2 have been derived from mutant enzyme activity data, phosphopeptide activation analysis, and the recent elucidation of the crystal structure of SHP-2 (17–19, 46–48). In the absence of an interacting tyrosine-phosphorylated binding partner for the SH2 domains, SHP-2 exists in a closed inactive conformation with the N-terminal SH2 domain plugging the catalytic center. Phosphopeptide occupation of the SH2 domains abrogates this interaction and leads to activation. Artificial activation occurs upon deletion of the N-terminal SH2 domain or both SH2 domains. Although the currently available structural data for SHP-1 do not allow direct conclusions about the role of the SH2 domains for activity regulation to be reached (49), the very similar overall architecture of SHP-1 and SHP-2, conservation of residues involved in the SH2 domain catalytic domain interaction in SHP-2 (19) in both molecules, and enzymatic data are in agreement with a similar mode of activation. When our binding data are considered, the most obvious explanation for the observed activation of both SHP-1 and SHP-2 by high concentrations of acidic phospholipids seems to be therefore that binding of these lipids through the SH2 domains leads to structural changes similar to phosphopeptide binding. Given the required high lipid concentrations for this effect, however, the physiological relevance of this lipid activation mechanism is questionable.

SHP-1 and SHP-2 exhibit a high degree of overall amino acid sequence homology except in the C-terminal tail where the degree of homology is only about 15%. Little is known about the function of the SHP-1 C-terminal tail. A role of the C-terminal tail has been reported for SHP-1 binding to the insulin receptor (22) *in vitro* but not to the EGF receptor (12). Deletion of parts of the C-terminus has been reported to lead to enzyme activation toward some artificial substrates, suggesting a role of the C-terminus in activity regulation or substrate recognition (18, 50, 51). Some of the published data are, however, controversial. In our hands, deletion of 41 C-terminal amino acids had no effect on activity toward pNPP or toward [ $^{32}$ P]Y-MBP at any pH that was tested (not shown). Activation by C-terminal deletions may depend in a subtle way on assay conditions. Also, most data reported hitherto were obtained with the hematopoietic variant of SHP-1, whereas we used the epithelial form of SHP-1 which possesses a somewhat different N-terminus (52). One could speculate that this form may have a higher basal activity and therefore cannot be activated by C-terminal deletions.

The available crystal structures of SHP-1 (49) and SHP-2 (19) do not contain the C-terminus of the enzymes, and therefore do not allow predictions about the possible role of the C-terminus for activity regulation. We have identified the C-terminus of SHP-1 as a high-affinity binding site for acidic phospholipids. Interestingly, this binding site in the C-terminus confers activation of SHP-1 toward the two substrates pNPP and [ $^{32}$ P]Y-MBP. The C-terminal sequence of SHP-1 contains three clusters of basic amino acids (amino acids 572–575, 578–583, and 595–597) which share similarities with the previously identified PA binding site in Raf-1 kinase (35). A GST fusion protein harboring SHP-1 amino acids 577–597 exhibited a clearly decreased DPPA binding activity, but DPPA binding was not completely lost (not shown). This finding renders unlikely the possibility that a single basic cluster is exclusively responsible for binding; however, analysis of point mutants will be necessary to fully clarify the contribution of individual sequence motifs to PA binding. PA fatty acid composition affected binding strength, in that PA species with saturated fatty acids (DPPA and distearoyl-PA, latter not shown) bound more avidly in the ELISAs than PA species from natural sources containing unsaturated fatty acids. It is currently unknown whether these differences are related to physiologically important specificities of the binding site on SHP-1 or more to the availability of PA for binding in particular types of assays as a result of physicochemical properties. PA identity used in previous studies for activation of SHP-1 has in most cases not been specified; however, it is likely that PA from natural sources has usually been used. This fact probably explains why, in previous studies, activation of SHP-1 toward pNPP has never been found as we observed it only with DPPA and not with PA derived from natural PC. With the macromolecular substrate [ $^{32}$ P]Y-MBP, activation was readily observed with PA from natural sources as well as with DPPA, and given the low concentrations required for activation, we were unable to discern possible differences in the potency of different PA species.

The mechanism of SHP-1 activation by C-terminal lipid binding is not clear. Lipid activation reduces the  $K_m$  toward pNPP and is observed at pH 6.3 and 7.4, i.e., under pH conditions where SHP-1 has very low activity (18). While C-terminal truncation abrogates activation via the C-terminal lipid binding site, activation of the truncated enzyme by a phosphopeptide binding partner is similar to that for the full-length enzyme. It seems tempting to speculate that lipid binding to the C-terminus of SHP-1 could lead to structural changes similar to phosphopeptide binding, facilitating substrate access to the active site. Monitoring these structural changes by spectroscopic methods in solution should be helpful in clarifying this point.

What may be the biological significance of the C-terminal lipid binding site of SHP-1? Given the reasonable affinity, PA may be a physiological ligand for the C-terminus of SHP-1. Interestingly, PIP3 also binds to the C-terminal lipid binding site and is capable of activating SHP-1. Lipid binding to the C-terminus of SHP-1 may contribute to activation and/or localization of SHP-1. Experiments are underway to test this concept in intact cells. The existence of this binding site clearly distinguishes SHP-1 from SHP-2 and predicts alternate ways of regulation. Although we were unable to observe activation of SHP-1 by C-terminal deletions, our finding of

SHP-1 activation via a C-terminal lipid binding site highlights a putative role of the SHP-1 C-terminus in activity regulation.

## ACKNOWLEDGMENT

We are grateful to Drs. A. Ullrich, R. Lammers, and D. Fujita for providing various cDNAs. We thank Mrs. Marit Müller for performing part of the PTP activity assays.

## REFERENCES

1. Tonks, N. K., and Neel, B. G. (1996) *Cell* 87, 365–368.
2. Neel, B. G., and Tonks, N. K. (1997) *Curr. Opin. Cell Biol.* 9, 193–204.
3. Adachi, M., Fischer, E. H., Ihle, J., Imai, K., Jirik, F., Neel, B., Pawson, T., Shen, S. H., Thomas, M., Ullrich, A., and Zhao, Z. Z. (1996) *Cell* 85, 15.
4. Feng, G. S., and Pawson, T. (1994) *Trends Genet.* 10, 54–58.
5. Ulyanova, T., Blasioli, J., and Thomas, M. L. (1997) *Immunol. Res.* 16, 101–113.
6. Barford, D., and Neel, B. G. (1998) *Structure* 6, 249–254.
7. Stein-Gerlach, M., Wallasch, C., and Ullrich, A. (1998) *Int. J. Biochem. Cell Biol.* 30, 559–566.
8. Shultz, L. D., Rajan, T. V., and Greiner, D. L. (1997) *Trends Biotechnol.* 15, 302–307.
9. Lorenz, U., Bergemann, A. D., Steinberg, H. N., Flanagan, J. G., Li, X., Galli, S. J., and Neel, B. G. (1996) *J. Exp. Med.* 184, 1111–1126.
10. Paulson, R. F., Vesely, S., Siminovitch, K. A., and Bernstein, A. (1996) *Nat. Genet.* 13, 309–315.
11. Chen, H. E., Chang, S., Trub, T., and Neel, B. G. (1996) *Mol. Cell. Biol.* 16, 3685–3697.
12. Tenev, T., Keilhack, H., Tomic, S., Stoyanov, B., Stein-Gerlach, M., Lammers, R., Krivtsov, A. V., Ullrich, A., and Böhmer, F. D. (1997) *J. Biol. Chem.* 272, 5966–5973.
13. Tomic, S., Greiser, U., Lammers, R., Kharitonov, A., Imyanitov, E., Ullrich, A., and Böhmer, F. D. (1995) *J. Biol. Chem.* 270, 21277–21284.
14. Klingmüller, U., Lorenz, U., Cantley, L. C., Neel, B. G., and Lodish, H. F. (1995) *Cell* 80, 729–738.
15. Neel, B. G. (1997) *Curr. Opin. Immunol.* 9, 405–420.
16. Jiao, H., Berrada, K., Yang, W., Tabrizi, M., Platanias, L. C., and Yi, T. (1996) *Mol. Cell. Biol.* 16, 6985–6992.
17. Lechleider, R. J., Sugimoto, S., Bennett, A. M., Kashishian, A. S., Cooper, J. A., Shoelson, S. E., Walsh, C. T., and Neel, B. G. (1993) *J. Biol. Chem.* 268, 21478–21481.
18. Pei, D., Lorenz, U., Klingmüller, U., Neel, B. G., and Walsh, C. T. (1994) *Biochemistry* 33, 15483–15493.
19. Hof, P., Pluskey, S., Dhe-Paganon, S., Eck, M. J., and Shoelson, S. E. (1998) *Cell* 92, 441–450.
20. Ottinger, E. A., Botfield, M. C., and Shoelson, S. E. (1998) *J. Biol. Chem.* 273, 729–735.
21. Vogel, W., Lammers, R., Huang, J., and Ullrich, A. (1993) *Science* 259, 1611–1614.
22. Uchida, T., Matozaki, T., Noguchi, T., Yamao, T., Horita, K., Suzuki, T., Fujioka, Y., Sakamoto, C., and Kasuga, M. (1994) *J. Biol. Chem.* 269, 12220–12228.
23. Brumell, J. H., Chan, C. K., Butler, J., Borregaard, N., Siminovitch, K. A., Grinstein, S., and Downey, G. P. (1997) *J. Biol. Chem.* 272, 875–882.
24. Zhao, Z. H., Shen, S. H., and Fischer, E. H. (1993) *Proc. Natl. Acad. Sci. U.S.A.* 90, 4251–4255.
25. Zhao, Z. Z., Larocque, R., Ho, W. T., Fischer, E. H., and Shen, S. H. (1994) *J. Biol. Chem.* 269, 8780–8785.
26. Liscovitch, M., and Cantley, L. C. (1994) *Cell* 77, 329–334.
27. Nishizuka, Y. (1995) *FASEB J.* 9, 484–496.
28. Franke, T. F., Kaplan, D. R., Cantley, L. C., and Toker, A. (1997) *Science* 275, 665–668.
29. Alessi, D. R., James, S. R., Downes, C. P., Holmes, A. B., Gaffney, P. R. J., Reese, C. B., and Cohen, P. (1997) *Curr. Biol.* 7, 261–269.
30. Hemmings, B. A. (1997) *Science* 277, 534.
31. Stephens, L., Anderson, K., Stokoe, D., Erdjument, B. H., Painter, G. F., Holmes, A. B., Gaffney, P. R., Reese, C. B., McCormick, F., Tempst, P., Coadwell, J., and Hawkins, P. T. (1998) *Science* 279, 710–714.
32. Toker, A., and Cantley, L. C. (1997) *Nature* 387, 673–676.
33. Nemoz, G., Sette, C., and Conti, M. (1997) *Mol. Pharmacol.* 51, 242–249.
34. Geng, D., Chura, J., and Roberts, M. F. (1998) *J. Biol. Chem.* 273, 12195–12202.
35. Ghosh, S., and Bell, R. M. (1997) *Biochem. Soc. Trans.* 25, 561–565.
36. Ghosh, S., Strum, J. C., Sciorra, V. A., Daniel, L., and Bell, R. M. (1996) *J. Biol. Chem.* 271, 8472–8480.
37. Tonks, N. K., Diltz, C. D., and Fischer, E. H. (1988) *J. Biol. Chem.* 263, 6722–6730.
38. Ranaka, A., and Fujita, D. J. (1986) *Mol. Cell. Biol.* 6, 3900–3909.
39. Keilhack, H., Tenev, T., Nyakatura, E., Godovac-Zimmermann, J., Nielsen, L., Seedorf, K., and Böhmer, F. D. (1998) *J. Biol. Chem.* 273, 24839–24846.
40. Bangham, A. D., Hill, M. W., and Miller, N. G. A. (1974) *Methods Membr. Biol.* 114, 1–68.
41. Ohki, S., and Arnold, K. (1990) *J. Membr. Biol.* 114, 195–203.
42. Köhler, G., Hering, U., Zschörnig, O., and Arnold, K. (1997) *Biochemistry* 36, 8189–8194.
43. Zheng, J., Cahill, S. M., Lemmon, M. A., Fushman, D., Schlessinger, J., and Cowburn, D. (1996) *J. Mol. Biol.* 255, 14–21.
44. Huang, C. L., Feng, S., and Hilgemann, D. W. (1998) *Nature* 391, 803–806.
45. El Bawab, S., Macovschi, O., Sette, C., Conti, M., Lagarde, M., Nemoz, G., and Prigent, A. F. (1997) *Eur. J. Biochem.* 247, 1151–1157.
46. Dechert, U., Adam, M., Harder, K. W., Clarklewis, I., and Jirik, F. (1994) *J. Biol. Chem.* 269, 5602–5611.
47. Sugimoto, S., Wandless, T. J., Shoelson, S. E., Neel, B. G., and Walsh, C. T. (1994) *J. Biol. Chem.* 269, 13614–13622.
48. Burshtyn, D. N., Yang, W. T., Yi, T. L., and Long, E. O. (1997) *J. Biol. Chem.* 272, 13066–13072.
49. Yang, J., Liang, X. S., Niu, T. Q., Meng, W. Y., Zhao, Z. Z., and Zhou, G. W. (1998) *J. Biol. Chem.* 273, 28199–28207.
50. Zhao, Z., Bouchard, P., Diltz, C. D., Shen, S. H., and Fischer, E. H. (1993) *J. Biol. Chem.* 268, 2816–2820.
51. Dechert, U., Affolter, M., Harder, K. W., Matthews, J., Owen, P., Clark, L. I., Thomas, M. L., Aebersold, R., and Jirik, F. R. (1995) *Eur. J. Biochem.* 231, 673–681.
52. Banville, D., Stocco, R., and Shen, S. H. (1995) *Genomics* 27, 165–173.
53. Shen, S. H., Bastien, L., Posner, B. I., and Chretien, P. (1991) *Nature* 352, 736–739.

BI982586W